Journal of Zhejiang University SCIENCE A
ISSN 1009-3095 (Print); ISSN 1862-1775 (Online)
www.zju.edu.cn/jzus; www.springerlink.com
E-mail: jzus@zju.edu.cn

Heat transfer and parametric studies of an encapsulated phase change material based cool thermal energy storage system

CHERALATHAN M.[†1], VELRAJ R.[2], RENGANARAYANAN S.[2]

([1]*School of Mechanical Engineering, S.R.M. Engineering College, SRM University, Kattankulathur, Chennai 603203, Tamilnadu, India*)

([2]*Institute for Energy Studies, Anna University, Chennai 600025, India*)

[†]E-mail: cheralathanm@yahoo.co.in

Received Apr. 4, 2006; revision accepted Aug. 21, 2006

Abstract: This work investigates the transient behaviour of a phase change material based cool thermal energy storage (CTES) system comprised of a cylindrical storage tank filled with encapsulated phase change materials (PCMs) in spherical container integrated with an ethylene glycol chiller plant. A simulation program was developed to evaluate the temperature histories of the heat transfer fluid (HTF) and the phase change material at any axial location during the charging period. The results of the model were validated by comparison with experimental results of temperature profiles of HTF and PCM. The model was also used to investigate the effect of porosity, Stanton number, Stefan number and Peclet number on CTES system performance. The results showed that increase in porosity contributes to a higher rate of energy storage. However, for a given geometry and heat transfer coefficient, the mass of PCM charged in the unit decreases as the increase in porosity. The *St* number as well as the *Ste* number is also influential in the performance of the unit. The model is a convenient and more suitable method to determine the heat transfer characteristics of CTES system. The results reported are much useful for designing CTES system.

Key words: Cool thermal energy storage (CTES), Energy storage, Freezing, Phase change materials (PCMs), Heat transfer analysis, Refrigeration

doi:10.1631/jzus.2006.A1886 **Document code:** A **CLC number:** O343.2

INTRODUCTION

Cool thermal energy storage (CTES) using the latent heat concept as an alternative to sensible heat storage offers a good option because of its high storage density and the nearly constant temperature heat removal characteristics during the discharging cycle. Since the principle of latent cool storage necessarily involves a change of state, heat transfer must occur in different modes depending on the state of charging and discharging. During the periods of low cooling demand the system removes heat from the thermal storage medium (water, phase change material, etc.) to be used latter to meet the air conditioning or process cooling load demand. One of the most popular latent heat storage systems is the encapsulated phase change material (PCM) system, which uses cylindrical geometries with or without fins, cans, plates or spherical capsules. This last seems to offer a number of advantages which make it among the most attractive methods of encapsulation. Arnold (1990), and Arnold and Eng (1991) investigated the freezing and melting characteristics of encapsulated ice storage system and described a numerical model. Dynamic model was used to simulate the phase change process and the effects of nonlinear heat transfer between the chilling fluid and capsule contents and also the performance of system during ice-building. Chen and Yue (1991a; 1991b), and Chen *et al*.(2000) developed a general lump model to predict the thermal performance of a cold storage system. They also conducted a series of experiments to investigate the effects of the inlet coolant temperature flow rate on nucleation of capsules, heat transfer and pressure drop of the tank during charging process utilizing cylindrical capsules. The heat transfer characteristics of cool thermal storage unit during the charging period were studied with 2 wt.% of sodium sulfate decahy-

drate (Na_2SO_4) in aqueous solution as the PCM by Ryu *et al*.(1991). Bedecarrats *et al*.(1996) studied the crystallization process of an organic eutectic in a spherical encapsulation.

Several investigators studied theoretically and experimentally the performance of thermal energy storage employing paraffin as PCM. Most reported in literature research on the latent heat storage (LHS) system was done for solar energy applications. The various heat transfer enhancement methods for LHS systems for domestic hot water applications and heat transfer characteristics of PCM during solidification were investigated by Velraj *et al*.(1997; 1999). Barba and Spiga (2003) analysed the behaviour of encapsulated salt hydrates used as PCM in a heat transfer system of a domestic hot water tank employing three different geometrical configurations of the PCM containers. Their study showed that spherical capsules have the largest energy density and the most rapid charge and release times, when compared against the slab or the cylindrical geometry. Ismail and Stuginsky (1999) presented a comparative study on six possible models for fixed bed storage systems for PCM and sensible heat storage. The models were first evaluated in relation to the computational time consumed to solve a specific test problem. The models were then compared in relation to the influence of particle size, void fraction, particle material, flow rate variations, heat transfer fluid (HTF) inlet temperature variations. Laboratory grade paraffin waxes have been tried as PCMs for cool storage (He and Setterwall, 2002; Cho and Choi, 2000).

A very limited number of studies were found on the cool thermal energy storage (CTES) in spherical capsules. The dynamic behaviour of a single spherical element used in the bed of thermal (ice) storage system was investigated by Adref and Eames (2002), and Eames and Adref (2002). Ismail and Henriquez (2002) presented a numerical model to simulate the process of heat transfer (charging and discharging) in an LHS system of packed bed of spherical capsules filled with PCM. The effect of HTF (ethylene glycol) entry temperature, the mass flow rate and material of the spherical capsule on the performance of the storage unit were investigated numerically and experimentally. Omari and Dumas (2004) presented an enthalpic modelling of the phase change inside the nodule coupled with a CFD simulation of the external flow to describe the mutual influence of the natural convection and the kinetics of crystallization. They also predicted the heat flux distribution on the surface of the nodule. Bilir and Ilken (2005) investigated the inward solidification problem of a PCM encapsulated in a cylindrical and spherical container and derived some correlations to predict the dimensionless total solidification time of the PCM in terms of Stefan number, Biot number and superheat parameter. Kousksou *et al*.(2005) developed a 2D model to study the influence of supercooling and the position of storage tank. They found that the optimum running of charging mode is obtained in the case of vertical position where the motions due to natural convection are in the same direction as the forced convection.

The latent cool storage system having many advantages is not in commercial use in industrial refrigeration and air conditioning applications so much as sensible cool storage system mainly because of the difficulty involved in the charging and discharging of cool energy from the storage system. In latent cool storage units, during phase change, the solid-liquid interface moves away from the convective heat transfer surface. In this process, the surface heat transfer rate decreases due to the increasing thermal resistance of the growing layer of frozen/molten medium. Understanding the heat transfer behavior during phase change in storage system is extremely important for the design of efficient storage systems. A number of researchers studied the thermal performance of latent heat thermal energy storage systems for solar energy storage and ice storage in air conditioning applications. However, the research work on combined sensible and latent cool thermal energy storage systems is still rarely in reported literatures.

This paper reports the results of a numerical heat transfer analysis on the encapsulated PCM based cool thermal energy storage integrated with refrigeration system. Parametric studies were carried out to analyze the effect of porosity and various non-dimensional parameters, such as Stanton number, Stefan number and Peclet number during charging process. The solid PCM fraction and energy stored in combined cool thermal energy storage system is reported.

NUMERICAL MODEL

The physical system under study is shown in Fig.1. It consists of cylindrical cool thermal energy

storage (CTES) tank integrated with refrigeration loop. The phase change material (water with super-cooling release additive) is encapsulated in spherical capsules packed in the insulated cylindrical storage tank. The system involves four flow circuits. The first circuit is the circulation of refrigerant (R134a) in the normal vapour compression cycle. The second circuit involves the charging mode, during which the HTF (30 wt.% aqueous ethylene glycol) from evaporator tank flows over the spherical capsules in the CTES tank. The HTF circulation is maintained by using a pump (P_1) and exchanges cold energy with the PCM capsules and transfers the heat to the evaporator in a refrigeration system during the charging mode. The third circuit involves the discharging mode, during which the refrigeration system is not in operation. The HTF passes through the storage medium at temperature higher than the PCM fusion temperature and receives the cold energy. Energy release from the storage tank is controlled by flow control valves (V_5 and V_6). The fourth circuit involves the direct mode in which no HTF flows through the CTES tank. During this direct production valve V_1 regulates the HTF flow to provide the required cooling. In the present analysis, only the charging mode is considered for discussion.

In order to investigate the CTES system performance, the mathematical formulation was made by establishing the energy balance at appropriate region of interest separately for the PCM in spherical capsules and the HTF. In the beginning of the charging process, the PCM temperature inside the packed capsules is higher than the freezing temperature. Cold energy from the HTF is stored inside the capsules by sensible heat until the PCM reaches its freezing temperature. As the charging process proceeds the cool storage is achieved by freezing the PCM at a constant temperature.

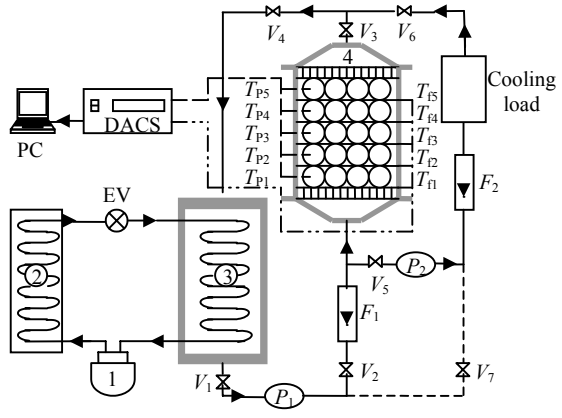

Fig.1 Layout of CTES tank integrated with refrigeration system

1: Compressor; 2: Condenser; 3: Evaporator tank; 4: CTES tank; DACS: Data acquisition and control system; EV: Expansion valve; F_1, F_2: Flow meter; P_1, P_2: Circulation pump; PC: Personal computer; T_f, T_p: Temperature sensors (RTDs); V_1~V_7: Flow control valves

Finally, the solid PCM becomes sub cooled. The cold energy is then stored in the solid PCM as sensible heat. The charging process is continued until thermal equilibrium is attained between HTF and PCM temperature. Therefore three time domains (sensible cooling of liquid PCM, latent cool storage, sensible cooling of solid PCM) are considered in order to simplify the analysis.

The following assumptions are made in the numerical analysis as they have very negligible effect for temperature variation inside the storage tank: (1) The HTF flow is fully developed; (2) The storage tank is well insulated; (3) The PCM and HTF thermophysical properties are constant; (4) The internal heat transfer coefficient between the capsules and the HTF is assumed to remain invariable during the charging mode; (5) There are no free convection effects.

Based on these assumptions, a general formulation of energy balance is established at the respective regions of the HTF and PCM separately and the following governing equations were obtained.

Governing equations and boundary conditions

The equations for the first time domain (sensible cooling of liquid PCM) are formulated as given below:

(1) For heat transfer fluid

An energy balance equation is obtained for the control volume (C.V.) considered in the CTES tank having cross sectional area A_C, and a height L during sensible cooling of the liquid PCM.

$$Q_x+hA_S(T_p-T_f)=Q_{x+dx}+\varepsilon\rho_f c_f A_C L\frac{\partial T_f}{\partial t}+\frac{\partial}{\partial x}m_f c_f T_f L. \tag{1}$$

In Eq.(1) the first term on the left hand side represents the energy entering the C.V. and the second term represents the energy transferred by convection from the HTF to the PCM. The three terms on the right hand side represent energy leaving the C.V., the HTF rate of change of internal energy and energy change

due to flow of HTF in the C.V. respectively. After simplification and rearrangement the following equation was obtained:

$$hA_S(T_p - T_f) + k_f A_C L \frac{\partial^2 T_f}{\partial x^2} = \varepsilon A_C L \rho_f c_f \left(\frac{\partial T_f}{\partial t} + u \frac{\partial T_f}{\partial x} \right), \tag{2}$$

where A_S is the wetted capsule area for storage volume, h is internal heat transfer coefficient, k_f is thermal conductivity of HTF, T_p and T_f is temperature of PCM and HTF respectively, ε is porosity, ρ_f is density of HTF, c_f is specific heat of HTF and u is velocity.

(2) For phase change material

$$k_p A_C L \frac{\partial^2 T_p}{\partial x^2} = (1-\varepsilon) A_C L \rho_p c_p \frac{\partial T_p}{\partial t} + hA_S(T_p - T_f). \tag{3}$$

where ρ_p is density of PCM and c_p is specific heat of PCM. Eq.(3) represents the net rate of change of heat by conduction in the PCM is equal to the rate of change of internal energy in the PCM and heat convected out to the HTF.

The initial and boundary conditions are

$$\begin{aligned} &T_f(t=0) = T_{fi};\ T_p(t=0) = T_{pi};\ 0 \le x \le L, \\ &x = 0,\ T_f = T_{f,in};\ \frac{\partial T_p}{\partial x} = 0 \text{ (for all } t), \\ &x = L,\ \frac{\partial T_f}{\partial x} = 0;\ \frac{\partial T_p}{\partial x} = 0 \text{ (for all } t), \end{aligned} \tag{4}$$

where T_{fi} and T_{pi} is the initial temperature of HTF and PCM respectively, $T_{f,in}$ is the temperature of HTF at inlet.

The equation for the second domain (latent cool storage) are formulated as shown below:

(1) For heat transfer fluid

Eq.(2) holds good with T_p=T_s

$$hA_S(T_s - T_f) + k_f A_C L \frac{\partial^2 T_f}{\partial x^2} = \varepsilon A_C L \rho_f c_f \left(\frac{\partial T_f}{\partial t} + u \frac{\partial T_f}{\partial x} \right). \tag{5}$$

(2) For phase change material

$$\frac{\partial}{\partial t}(m_{sol} \cdot \lambda) = hA_S(T_{ps} - T_f), \tag{6}$$

where λ is latent heat of solidification, T_{ps} is temperature of PCM at solid state. Eq.(6) represents the rate of change of PCM latent cool energy is equal to the heat convected out to the HTF.

The initial conditions in this time domain are

$$T_f(t = t_s) = T_{fs};\ T_p(t = t_s) = T_{ps};\ m_{sol}(t = t_s) = 0. \tag{7}$$

In the third time domain (sensible cooling of solid PCM), Eqs.(2) and (3) are applicable with properties of liquid PCM replaced by those of solid PCM.

Nondimensional equations

All the above equations were non-dimensionalized through the following parameters

$$\begin{aligned} &\theta = \frac{T - T_{f,in}}{T_{pi} - T_S},\ \tau = \frac{t}{t_c},\ t_c = \frac{L}{u},\ x^+ = \frac{x}{L}, \\ &R_{kl} = \frac{k_l}{k_f},\ R_{cl} = \frac{(1-\varepsilon)\rho_l c_l}{\varepsilon \rho_l c_l},\ R_{cs} = \frac{(1-\varepsilon)\rho_s c_s}{\varepsilon \rho_f c_f}, \\ &St = \frac{hA_S}{\varepsilon u \rho_f c_f},\ Ste = \frac{c_l(T_{pi} - T_s)}{\lambda},\ Pe = \frac{\varepsilon u \rho_f c_f L}{k_f}, \end{aligned} \tag{8}$$

where the dimensionless parameter t_c stands for the characteristic time of the system, R_{kl} is the water-to-fluid conductivity ratio, R_{cl} is the effective heat capacity ratio of the water and the coolant, *Ste* is the Stefan number, *St* is the Stanton number, and *Pe* is the Peclet number.

The non-dimensional equations in the first time domain for HTF and PCM are:

(1) For HTF:

$$\frac{\partial \theta_f}{\partial \tau} + \frac{\partial \theta_f}{\partial x^+} = \frac{1}{Pe} \frac{\partial^2 \theta_f}{\partial x^{+2}} + St(\theta_p - \theta_f). \tag{9}$$

(2) For PCM:

$$\frac{\partial \theta_p}{\partial \tau} = \frac{1}{Pe} \frac{R_{kl}}{R_{cl}} \frac{\partial^2 \theta_p}{\partial x^{+2}} - \frac{St}{R_{cl}}(\theta_p - \theta_f). \tag{10}$$

The initial and boundary conditions for Eqs.(9) and (10) are

$$\begin{aligned} &\theta_f(\tau = 0) = \theta_{fi};\ 0 < x^+ < 1; \\ &\theta_p(\tau = 0) = \theta_{pi};\ 0 < x^+ < 1; \end{aligned}$$

$$x^+=0,\ \theta_f=\theta_{f,in};\ \frac{\partial\theta_p}{\partial x^+}=0 \text{ (for all } \tau);$$

$$x^+=1,\ \frac{\partial\theta_f}{\partial x^+}=0;\ \frac{\partial\theta_p}{\partial x^+}=0 \text{ (for all } \tau). \quad (11)$$

In the second time domain the PCM inside the capsules reaches the freezing state (i.e. $\theta_p=\theta_{ps}$), solidification process begins. The cool energy is stored by freezing the PCM at a constant temperature. Part of the capsules is in the liquid state and part in the solid state. The energy equation for the PCM capsules and the HTF can be written as,

$$\frac{\partial\beta}{\partial\tau}=\frac{St\ Ste}{R_{cl}}(\theta_{ps}-\theta_f), \quad (12)$$

where solidified mass fraction $\beta=\dfrac{m_{sol}}{(1-\varepsilon)\rho_l A_c L}$ and *Ste* is the ratio of the PCM sensible heat content in the capsule to the PCM latent heat of solidification.

$$\frac{\partial\theta_f}{\partial\tau}+\frac{\partial\theta_f}{\partial x^+}=\frac{1}{Pe}\frac{\partial^2\theta_f}{\partial x^{+2}}+St(\theta_{ps}-\theta_f). \quad (13)$$

The initial conditions in this time domain are

$$\beta(\tau=\tau_s)=0;\ \theta_f(\tau=\tau_s)=\theta_{fs};\ \theta_p(\tau=\tau_s)=\theta_{ps}. \quad (14)$$

In the final stage of cool storage, cool energy is stored in the sub cooled solid state. The governing equation in this time domain is the same as that in the first time domain except that the liquid PCM properties are replaced by solid PCM properties.

Energy stored in CTES system

The instantaneous and cumulative cool energy stored are calculated from the values of HTF temperatures at the storage tank inlet and outlet. The total energy stored in the form of both sensible and latent cool energy can be obtained in the non-dimensional form by the following equation.

$$Q^*=\frac{\int_0^t m_f c_f(T_f-T_{f,in})\mathrm{d}t}{m_f c_f(T_{pi}-T_s)t_c}=\int_0^t\theta_f\mathrm{d}\tau. \quad (15)$$

Computational procedure

The model for the CTES system during the charging mode has been completely developed with the governing equations being considered in terms of non-dimensional quantities. The above equations were discretized employing fully implicit finite difference scheme and the resulting algebraic equations are solved using Gauss-Seidel iterative technique considering the suitable equations concerned for each time domain. The program has been written in C language and tested for different time steps. The step size of $\Delta\tau$=0.01 was found suitable and the variation of step size beyond the value led a more computational time and sometimes non convergence.

EXPERIMENTAL SETUP AND INSTRUMENTATION

A vertical CTES tank has been integrated with the evaporator of vapour compression refrigeration system using R134a as refrigerant. The photographic view of the experimental setup is shown in Fig.2. In the evaporator cold energy is transferred to the HTF and a temperature controller is attached to it, which can maintain the HTF temperature at any desired constant temperature between 0 °C to −20 °C during the charging process. The evaporator tank is insulated with 50 mm thick polyurethane foams (PUF). The PCM is filled in the spherical capsules of 48 mm diameter (*d*). The capsules are made of high density polyethylene material. The maximum number (*N*) of spherical capsules in the tank was 250. The PCM inside each capsule was 50 g of distilled water with heterogeneous nucleation agents. Adding nucleation agents initiate the freezing of water at its melting temperature. The PCM capsules were filled with 90% volume to prevent the capsules from cracking due to thermal expansion during the phase change process. In the top and bottom of the cylindrical storage tank, perforated distributor plates were provided to achieve uniform flow distribution. A rotameter with accuracy of ±0.5% was installed in the flow line between the evaporator and storage tank to measure the flow rate of the aqueous ethylene glycol. RTDs (PT100) were used to measure the temperature of the refrigerant. The temperature of the HTF and the PCM temperature were measured using k-type thermocouples (with 1.5 mm o.d). Five thermocouples were positioned axially at 100 mm interval and six of them were positioned at radial location and interval of 60 mm.

Three thermocouples were inserted into the spherical capsules to measure the PCM temperatures. Also two thermocouples were provided at the inlet and outlet to measure the temperature of the HTF entering and leaving the storage tank. All the thermocouples and RTDs were connected with data acquisition system. A data acquisition and control system (AI 8000+) and a personal computer (Pentium IV) were used for data recording and storage.

Fig.2 Photographic view of the experimental setup

RESULTS AND DISCUSSION

The values of geometrical and input parameters are listed in Table 1. The aqueous solution of 30 wt.% ethylene glycol was used as heat transfer fluid and distilled water with heterogeneous nucleation agents (super cooling release additive) was used as PCM in the present analysis. The thermo-physical properties of HTF, PCM and also the values of other parameters employed in the present analysis are tabulated in Table 2. A complete analysis of the CTES unit has to consider the individual and collective influence of various parameters. The numerical results of the present model were used to study the influence of certain selected parameters on the performance of the unit. The discussion of results is focused on the effect of porosity, effect of Stefan number, Stanton number and Peclet number on CTES system performance. The results showed that the variation of *Pe* number has no influence on the HTF and PCM temperature histories so a plot of *Pe* number variations is not included in the present results and discussion.

Table 1 Geometrical and input parameters

Geometrical parameters		Input parameters	
L	500 mm	T_{pi}	15 °C
D	240 mm	T_{fi}	−10 °C
d	48 mm	m_f	9 kg/min
n	5		
N	250	ε	36.5%
	200		49%
	150		61%

Table 2 Thermo physical and other properties of PCM and HTF

Thermo physical properties		Other properties		Non-dimensional numbers	
c_f	3.65 kJ/(kg·K)	λ	333.6 kJ/kg	*Pe*	11.3, 22.5
c_p	4.186* kJ/(kg·K)	R_{cl}	4.0	*St*	0.5, 0.75, 1.0
	2.01** kJ/(kg·K)	R_{kl}	2.9	*Ste*	0.2, 0.4, 0.6
ρ_f	1045 kg/m^3	R_{cs}	1.7	−	−
ρ_p	1000* kg/m^3	R_{ks}	2.7	−	−
	920** kg/m^3	−	−	−	−
k_f	0.485 W/(m·K)	−	−	−	−
k_p	0.566* W/(m·K)	−	−	−	−
	2.22** W/(m·K)	−	−	−	−

* Liquid state; ** Solidification (or melting) state

Effect of porosity (ε)

Numerical calculations were done for various conditions of the experimental measurement in order to confirm the validity of the model and assumptions. In the theoretical analysis the values of the internal heat transfer coefficient in *St* number were estimated so that the numerical results would accord with experimental results.

Fig.3a shows the temperature histories of PCM under the conditions of ε=36%, m_f=3 kg/min, T_{fi}=−10 °C. In the numerical results the temperature values (T_{p1} to T_{p5}) were plotted at five different axial locations of the storage tank whereas in the experimental results the temperature values are shown only at three locations i.e., the PCM near the inlet (T_{p1}) at the middle (T_{p2}) and near the outlet (T_{p5}) of the spherical capsules kept inside the storage tank. The model results are in good agreement with the experimental results except at the final stage of freezing. During the first time domain the drop in temperature of the liquid PCM was very high due to the higher heat transfer rate that exists between the HTF and liquid PCM as the temperature difference between the HTF and the PCM was very high. With time, the PCM inside the capsules changes its phase with the temperature remaining constant. At the third time domain all the temperature decreased until they reached steady state.

Also it is noted from the figure that complete freezing of the spherical capsules in the bottom layer was less when compared to the other layers since the HTF enters at the bottom of the storage tank.

Fig.3b presents the temperature histories of the HTF at five different locations of the storage tank. The experimental results are also shown at the bottom (T_{f1}) and top (T_{f5}) of the storage tank to compare the results with the numerical model. It is seen from the figure that the results are in good agreement with the numerical model. So it is clear that the present 1D model can predict accurately the HTF and PCM temperature histories.

It is observed from Figs.3a and 3b that the PCM temperature is constant at all the layers whereas the temperature of HTF increases gradually from the bottom layer to the top layer of the storage tank. The HTF absorbs the heat when it comes into contact with the PCM capsules and the heat transfer rate is high in the bottom layer and decreases gradually when the HTF moves upward as the temperature difference decreases gradually. Hence the PCM in the bottom layer is frozen first and the PCM at the top layer is frozen at the end (Fig.3a).

To study the performance of the storage system at different porosities of the HTF, Fig.4 is drawn for ε=49% and ε=61% under the same HTF inlet temperature of −10 °C and flow rate of 9 kg/min respectively. It is observed from Figs.3 and 4 that lower porosity increases the charging time. Also the time for complete PCM freezing is very much less when ε was 61% and that it increases by 23% and 80% when ε was 49% and 36.5% respectively. Lower porosity value indicates higher heat capacity of the storage tank and hence the larger time required for freezing. For higher porosity, the maximum energy charged

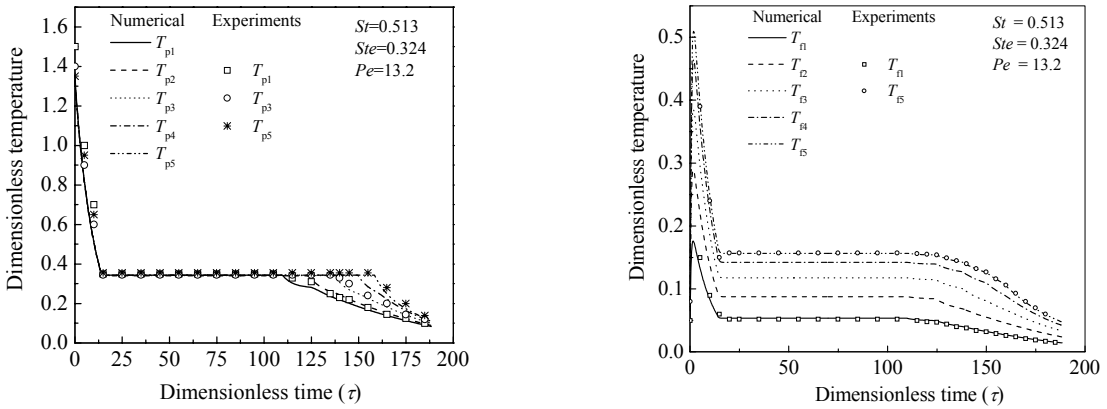

Fig.3 Temperature distributions of the phase change (a) and the heat transfer fluid (b) material at $T_{f,in}$=−10 °C (m_f=3 kg/min, ε=36%)

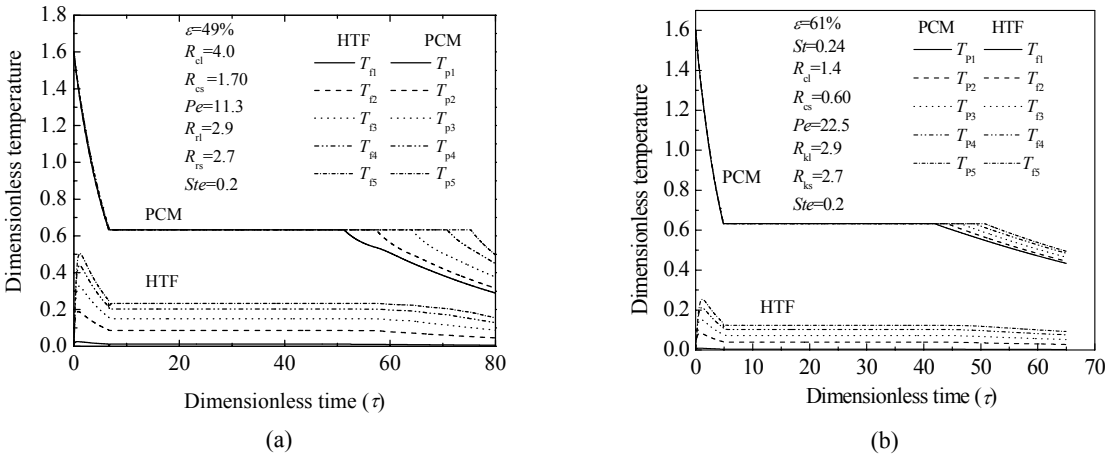

Fig.4 Temperature distributions of HTF and PCM. (a) ε=49%; (b) ε=61%

and charging time decreases. This is due to increase in porosity that would result in increased HTF passage and lower mass of PCM capsules in the entire storage tank.

Fig.5a shows the variation of solid fraction with dimensionless time during the charging process for different porosities. It was found that the time required for the start and completion of freezing decreases with increase in porosity. This illustrates that increase in HTF heat capacity results in decrease of the completion time for latent cool storage. The cool energy is stored in the form of combined sensible and latent cool energy. It was observed that more than 85% of energy was stored by PCM as latent cool energy and that the remaining was stored in PCM capsules and HTF as sensible cooling.

Fig.5b demonstrates the effect of porosity on dimensionless cool storage capacity (Q^*/Q_t^*) with dimensionless time. As the porosity value increases the time required for completion of storage decreases due to decrease in PCM volume in the storage tank. It was observed that, as the porosity increases from 36.5% to 49% the latent cool energy stored reduced to 20% and 40% for 61% porosity. The time required for completion of charging process was less when ε=61% and increases by 55% and 100% when ε=49% and 36.5% respectively.

Effect of Stanton number

Figs.6a and 7 present the temperature distributions of HTF and PCM, the solid fraction and cool storage capacity for various *St* numbers (*St*=0.5, 0.72, 1.0) in the top layer of cool thermal energy storage tank. Fig.6a shows the HTF and PCM temperature distribution at the top layer of the storage tank for various *St* number. It was observed that the variation

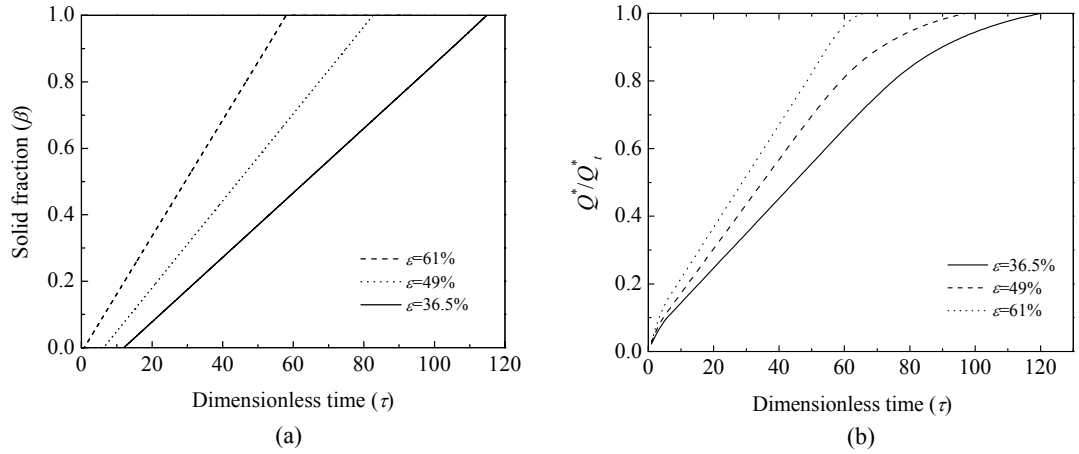

Fig.5 Variation of solid fraction (a) and energy stored (b) with dimensionless time at different porosities

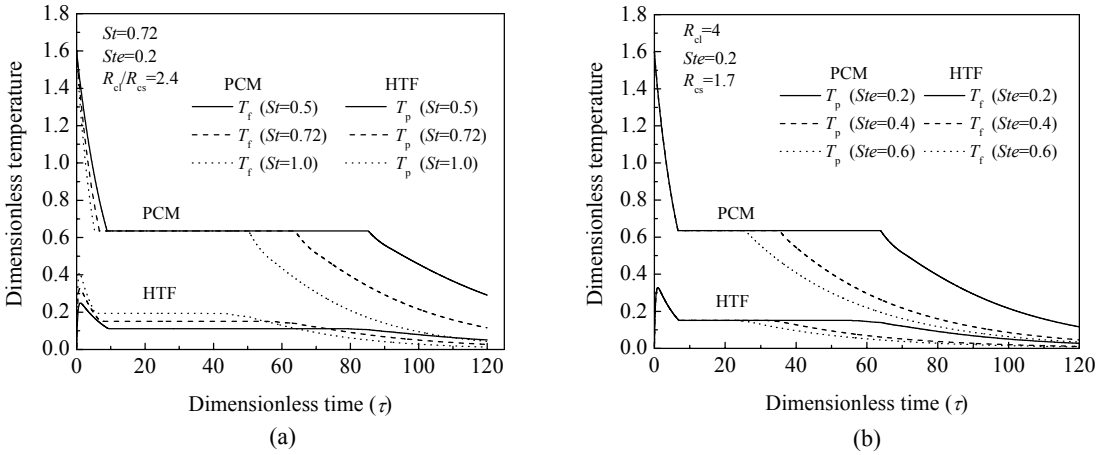

Fig.6 Temperature distributions of HTF and PCM for various *St* numbers (a) and *Ste* numbers (b)

of *St* number had large influence on the HTF temperature and did not have any effect on PCM capsules temperature during the phase change process. Fig.7a illustrates the solid fraction of PCM with dimensionless time for various *St* numbers. It can be seen that the time required for latent cool energy storage decreases with increase in *St* number. This is because increase in the *St* number increases the internal heat transfer coefficient. Fig.7b provides the instantaneous energy stored in cool storage with time for different *St* numbers. The time required for completion of charging process decreases to 20% when the *St* number varies from 0.5 to 0.75 and that 30% for *St* number is 0.5. As per the present results *St* number affects the HTF temperature and PCM temperatures, freezing rate and storage capacity of CTES system. Hence the effect of *St* number has great influence on the dynamic performances of the cool thermal storage system.

Effect of Stefan number

Figs.6b and 8 present the temperature distributions of HTF and PCM, and the solid fraction and cool storage capacity for various *Ste* numbers (*Ste*=0.2, 0.4 and 0.6). Fig.6b shows the variation of *Ste* number does not have any effect on the temperature profiles of the HTF and PCM during the sensible cooling of PCM capsules whereas the effect is quite large in the later part of the storage process. The solid fraction of PCM with time for various *Ste* number is shown in Fig.8a. The freezing of PCM is rapid when *Ste* number increases from 0.2 to 0.6. The *Ste* number related to thermal properties of the PCM and has greater influence on the storage capacity of CTES system.

Fig.8b illustrates the effect of *Ste* number on the instantaneous energy storage with dimensionless time and shows that the dimensionless time required for the completion of charging process is very minimal (τ=40) when *Ste*=0.6 and it increases by 38% and

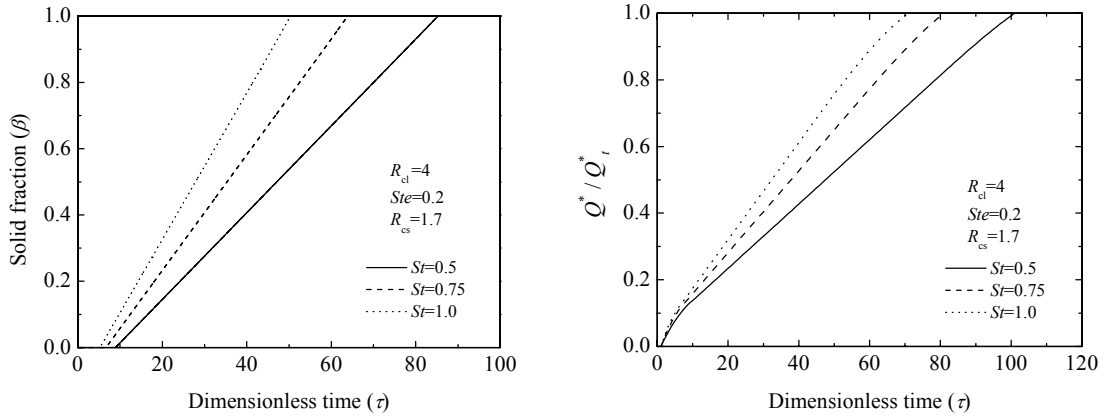

(a) (b)

Fig.7 Variation of solid fraction (a) and energy stored (b) with dimensionless time at different *St* numbers

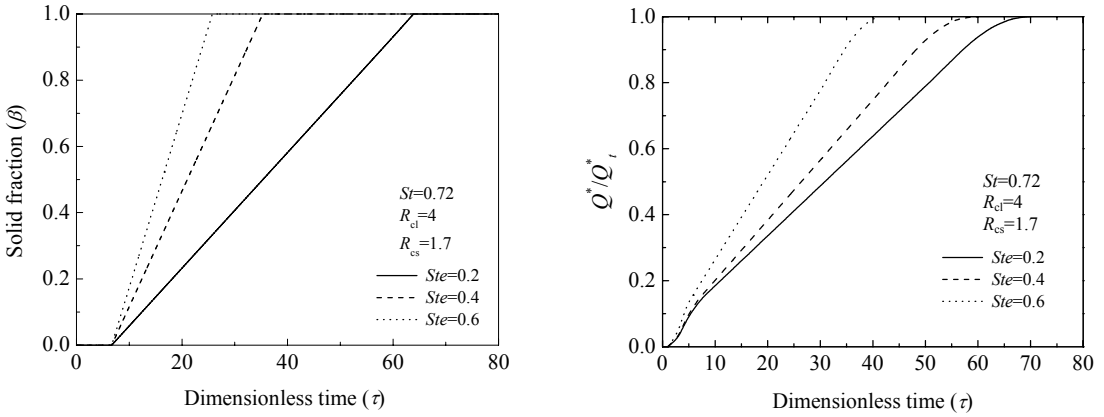

(a) (b)

Fig.8 Variation of solid fraction (a) and energy stored (b) with dimensionless time at different *Ste* numbers

62% when the *Ste* number was 0.4 and 0.2 respectively. The time required for completion of cool storage (charging process) increases with decrease in the *Ste* number.

CONCLUSION

In this paper the energy storage inside spherical packed capsules with a HTF flowing in the axial direction was analyzed numerically and experimentally. A simplified transient 1D model was developed to analyze the performance of combined cool thermal energy storage (CTES) system. The results showed that the model is a convenient and simple method to determine the heat transfer characteristics of combined CTES system. Three independent dimensionless parameters (*St*, *Ste* and *Pe*) characterizing the thermal performance of storage system were identified. Their effects on system performance were studied. The following conclusions can be drawn from the results:

(1) For lower porosity, the time required for freezing the PCM is longer than for higher porosity at constant HTF flow rate. This is due to increase porosity that would result in increased HTF passage and lower mass of PCM capsules in the entire storage tank. (2) The time required for latent heat energy storage and completion of charging process decreases with increase in *St* number and it decides the dynamic performance of the storage system. (3) The time required for completion of charging increase with decrease in the *Ste* number. The *Ste* number is mainly related to storage capacity, which is a static performance of the storage unit.

The storage systems designed for higher Stanton numbers (>0.5) and higher porosity (>0.49) take less time for energy charging for a given energy storage capacity whereas those systems designed for higher *Ste* number (>0.4) and higher porosity (>0.60) reduce the amount of energy storage in the system. Hence moderate values of *Ste* number (0.2~0.4), porosity (0.40~0.49) and higher values of Stanton number (0.7~1.0) are to be chosen for higher and faster energy storage while designing CTES systems.

References

Adref, K.T., Eames, I.W., 2002. Experiments on charging and discharging of spherical thermal (ice) storage elements. *Int. J. Energy Rese.*, **26**(11):949-964. [doi:10.1002/er.816]

Arnold, D., 1990. Dynamic simulation of encapsulated ice stores. Part I: the model. *ASHRAE Trans.*, **96**(1):1103-1110.

Arnold, D., Eng, C., 1991. Laboratory performance of an encapsulated ice store. *ASHRAE Trans.*, **97**(2):1245- 1254.

Barba, A., Spiga, M., 2003. Discharge mode for encapsulated PCMs in storage tanks. *Solar Energy*, **74**(2):141-148. [doi:10.1016/S0038-092X(03)00117-8]

Bedecarrats, J.P., Strub, F., Falcon, B., Dumas, J.P., 1996. Phase-change thermal energy storage using spherical capsules: performance of a test plant. *Int. J. Refrig.*, **19**(3):187-196. [doi:10.1016/0140-7007(95)00080-1]

Bilir, L., Ilken, Z., 2005. Total solidification time of a liquid phase change material enclosed in cylindrical/spherical containers. *Appl. Therm. Eng*., **25**(10):1488-1502. [doi:10.1016/j.applthermaleng.2004.10.005]

Chen, S.L., Chen, C.L., Tin, C.C., Lee, T.S., Ke, M.C., 2000. An experimental investigation of cold storage in an encapsulated thermal storage tank. *Experimental Thermal and Fluid Science*, **23**(3-4):133-144. [doi:10.1016/S0894-1777(00)00045-5]

Chen, S.L., Yue, J.S., 1991a. Thermal performance of cool storage in packed capsules for air conditioning. *Heat Recovery Systems & CHP*, **11**(6):551-561. [doi:10.1016/0890-4332(91)90057-B]

Chen, S.L., Yue, J.S., 1991b. A simplified analysis for cold storage in porous capsules with solidification. *ASME J. Energy Resour. Technol.*, **113**:108-116.

Cho, K., Choi, S.H., 2000. Thermal characteristics of paraffin in a spherical capsule during freezing and melting processes. *Int. J. Heat Mass and Transfer*, **43**(17):3183-3196. [doi:10.1016/S0017-9310(99)00329-4]

Eames, I.W., Adref, K.T., 2002. Freezing and melting of water in spherical enclosures of the type used in thermal (ice) storage systems. *Appl. Therm. Eng.*, **22**(7):733-745. [doi:10.1016/S1359-4311(02)00026-1]

He, B., Setterwall, F., 2002. Technical grade paraffin waxes as phase change materials for cool thermal storage and cool storage systems capital cost estimation. *Energy Conversion and Management*, **43**(13):1709-1723. [doi:10.1016/S0196-8904(01)00005-X]

Ismail, K.A.R., Henriquez, J.R., 2002. Numerical and experimental study of spherical capsules packed bed latent heat storage system. *Appl. Therm. Eng.*, **22**(15):1705-1716. [doi:10.1016/S1359-4311(02) 00080-7]

Ismail, K.A.R., Stuginsky, R., 1999. A parametric study on possible fixed bed models for PCM sensible heat storage. *Appl. Therm. Eng.*, **19**(7):757-788. [doi:10.1016/S1359-4311(98)00081-7]

Kousksou, T., Bedecarrats, J.P., Dumas, J.P., Mimet, A., 2005. Dynamic modelling of the storage of an encapsulated ice tank. *Appl. Therm. Eng*., **25**(10):1534-1548. [doi:10.1016/j.applthermaleng.2004.09.010]

Omari, K.E., Dumas, J.P., 2004. Crystallization of supercooled spherical nodules in a flow. *Int. J. Thermal Sciences*, **43**(12):1171-1180. [doi:10.1016/j.ijthermalsci.2004.04.007]

Ryu, H.W., Hong, S.A., Shin, B.C., Kim, S.D., 1991. Heat transfer characteristics of cool thermal storage systems. *Energy*, **16**(4):727-737. [doi:10.1016/0360-5442(91)90022-E]

Velraj, R., Seeniraj, R.V., Hafner, B., Faber, C., Schwarzer, K., 1997. Experimental analysis and numerical modelling of inward solidification on a finned vertical tube for a latent heat storage unit. *Solar Energy*, **60**(5):281-290. [doi:10.1016/S0038-092X(96)00167-3]

Velraj, R., Seeniraj, R.V., Hafner, B., Faber, C., Schwarzer, K., 1999. Heat transfer enhancement in a latent heat storage system. *Solar Energy*, **65**(3):171-180. [doi:10.1016/S0038-092X(98)00128-5]